A molecular link between cell wall biosynthesis, translation fidelity, and stringent response in *Streptococcus pneumoniae*

Surya D. Aggarwal[a,1], Adrian J. Lloyd[b,2], Saigopalakrishna S. Yerneni[c], Ana Rita Narciso[d,e], Jennifer Shepherd[b], David I. Roper[b], Christopher G. Dowson[b], Sergio R. Filipe[d,e,2], and N. Luisa Hiller[a,2]

[a]Department of Biological Sciences, Carnegie Mellon University, Pittsburgh, PA 15213; [b]School of Life Sciences, University of Warwick, Coventry CV4 7AL, United Kingdom; [c]Department of Biomedical Engineering, Carnegie Mellon University, Pittsburgh, PA 15213; [d]Laboratory of Bacterial Cell Surfaces and Pathogenesis, Instituto de Tecnologia Química e Biológica António Xavier, Universidade Nova de Lisboa, 1099-085 Oeiras, Portugal; and [e]Unidade de Ciências Biomoleculares Aplicadas (UCIBIO), Departamento de Ciências da Vida, Faculdade de Ciências e Tecnologia, Universidade Nova de Lisboa, 2825-149 Caparica, Portugal

Edited by Susan Gottesman, NIH, Bethesda, MD, and approved February 15, 2021 (received for review August 31, 2020)

Survival in the human host requires bacteria to respond to unfavorable conditions. In the important Gram-positive pathogen *Streptococcus pneumoniae*, cell wall biosynthesis proteins MurM and MurN are tRNA-dependent amino acyl transferases which lead to the production of branched muropeptides. We demonstrate that wild-type cells experience optimal growth under mildly acidic stressed conditions, but Δ*murMN* strain displays growth arrest and extensive lysis. Furthermore, these stress conditions compromise the efficiency with which alanyl-tRNA^{Ala} synthetase can avoid noncognate mischarging of tRNA^{Ala} with serine, which is toxic to cells. The observed growth defects are rescued by inhibition of the stringent response pathway or by overexpression of the editing domain of alanyl-tRNA^{Ala} synthetase that enables detoxification of tRNA misacylation. Furthermore, MurM can incorporate seryl groups from mischarged Seryl-tRNA$^{Ala}_{UGC}$ into cell wall precursors with exquisite specificity. We conclude that MurM contributes to the fidelity of translation control and modulates the stress response by decreasing the pool of mischarged tRNAs. Finally, we show that enhanced lysis of Δ*murMN* pneumococci is caused by LytA, and the *murMN* operon influences macrophage phagocytosis in a LytA-dependent manner. Thus, MurMN attenuates stress responses with consequences for host–pathogen interactions. Our data suggest a causal link between misaminoacylated tRNA accumulation and activation of the stringent response. In order to prevent potential corruption of translation, consumption of seryl-tRNA^{Ala} by MurM may represent a first line of defense. When this mechanism is overwhelmed or absent (Δ*murMN*), the stringent response shuts down translation to avoid toxic generation of mistranslated/misfolded proteins.

Streptococcus pneumoniae | cell wall | translation quality control | stringent response | autolysis

Gram-positive bacteria have evolved a thick and sophisticated cell wall that ensures bacterial structural integrity and is critical for cellular viability. This dynamic structure includes peptidoglycan, surface anchored proteins, wall teichoic acids, lipoteichoic acids, lipoproteins, and capsular polysaccharides (1, 2). It is also a major target of immune defenses and antibiotics (3, 4). Bacteria with high pathogenic potential, such as *Streptococcus pneumoniae* (pneumococcus), encounter hostile environments within the human host, where the cell wall serves as a barrier and an interface between the bacterium and its host.

The pneumococcal peptidoglycan consists of glycan chains that are cross-linked directly or indirectly via peptide bridges (5). These glycan chains consist of alternating *N*-acetylglucosamine (NAG) and *N*-acetylmuramic acid (NAM) residues. Each NAM subunit is attached to a stem peptide which is cross-linked to an adjacent stem peptide from a nearby glycan chain. In the pneumococcus, this cross-link can be direct or indirect through a dipeptide branch that is assembled by MurM and MurN, two transfer RNA (tRNA)-dependent amino acyl transferases (6, 7). Indirect cross-linking requires the synthesis of lipid II-linked branched peptidoglycan precursors on the cytoplasmic face of the pneumococcal cell membrane. MurM transfers alanyl or seryl residues from aminoacyl-tRNAs to the ε-amino group of the stem peptide lysine of the peptidoglycan precursor lipid II (6), and MurN appends an alanyl residue from alanyl-tRNA^{Ala} to the residue added by MurM (7). Lipid precursors are then flipped to the extracellular face of the cell membrane to be polymerized by transglycosylation. The nascent glycan strands are then cross-linked through the third residue (L-Lys, which can be branched or unbranched) of a stem peptide emanating from one glycan strand to the fourth residue (D-Ala) of the stem peptide of an adjacent glycan strand by penicillin binding proteins (8, 9). Thus, pneumococcal peptidoglycan synthesis links stem peptides with a dipeptide comprising a C-terminal L-Ala or L-Ser and an N-terminal L-Ala.

Significance

During infection, microbes must survive the hostile environmental conditions of the human host. When exposed to stresses, bacteria activate an intracellular response, known as the stringent response pathway, to ensure their survival. This study connects two fundamental pathways important for cellular growth in a Gram-positive pathogen: it demonstrates that enzymes responsible for cell wall biosynthesis are connected to the stringent response pathway via their ability to ameliorate errors in protein translation. Our study was performed on *S. pneumoniae*, where the MurM cell wall biosynthesis enzyme, a tRNA-dependent amino acyl transferase, is linked to penicillin resistance. We now demonstrate the importance of MurM in translation quality control and establish that it serves as a gatekeeper of the stringent response pathway.

Author contributions: S.D.A., D.I.R., C.G.D., S.R.F., and N.L.H. designed research; S.D.A., A.J.L., S.S.Y., A.R.N., J.S., and S.R.F. performed research; S.D.A., A.J.L., and S.R.F. contributed new reagents/analytic tools; S.D.A., A.J.L., S.S.Y., A.R.N., J.S., D.I.R., C.G.D., S.R.F., and N.L.H. analyzed data; and S.D.A., A.J.L., and N.L.H. wrote the paper.

The authors declare no competing interest.

This article is a PNAS Direct Submission.

[1]Present address: Department of Microbiology, New York University Grossman School of Medicine, New York, NY 10016.

[2]To whom correspondence may be addressed. Email: adrian.lloyd@warwick.ac.uk, sfilipe@fct.unl.pt, or lhiller@andrew.cmu.edu.

This article contains supporting information online at https://www.pnas.org/lookup/suppl/doi:10.1073/pnas.2018089118/-/DCSupplemental.

Published March 30, 2021.

Allelic variants of *murM* lead to diversity in the nature of stem peptide branching in the cell wall peptidoglycan (10–12). Similarly, allelic variation among pneumococcal penicillin binding protein genes is responsible for drastically increasing the minimum inhibitory concentration for β-lactam antibiotics. However, such clinical high-level resistance to β-lactams additionally requires *murMN* as inactivation of this operon leads to a complete loss of penicillin resistance (8, 13).

The employment of aminoacyl-tRNAs as MurM and MurN substrates juxtaposes the fundamental cellular functions of peptidoglycan biosynthesis and protein translation with each other and antibiotic resistance. The ability of MurM to incorporate both seryl and alanyl residues from tRNA into peptidoglycan branches is intriguing. Serine is an amino acid that is erroneously recognized by alanyl-tRNA^{Ala} synthetase (AlaRS), which itself possess editing mechanisms to forestall noncognate seryl-tRNA^{Ala} synthesis and consequent misincorporation of serine at alanine codons (14, 15).

In vitro, MurM can deacylate seryl and alanyl-tRNA^{Ala} by hydrolysis (6, 16). This led to the hypothesis that MurM-catalyzed aminoacyl-tRNA deacylation provides an *in trans* mechanism for the correction of deficits in the editing activity and fidelity of AlaRS (16). However, several observations are inconsistent with the role of MurM in editing misacylation of tRNA via simple hydrolytic deacylation of a mischarged substrate: 1) initial reports were made with a vast excess of enzymes relative to the tRNA substrate which precluded demonstration of MurM catalysis (16), 2) MurM-supported aminoacyl-tRNA hydrolysis rates are negligible when compared with those of peptidoglycan precursor aminoacylation (6), and 3) MurM-mediated alanyl-tRNA^{Ala} deacylation is significantly more rapid than seryl-tRNA^{Ala} deacylation (16). Therefore, the tantalizing possibility that seryl-tRNA^{Ala} consumption by MurM-catalyzed lipid II serylation contributes to maintaining accuracy of alanine codon translation remains to be validated in the literature.

Under stress, many bacterial cellular processes including translation are regulated by the stringent response pathway. Deprivation of amino acids or carbon sources, elevated temperature, and acidic conditions can trigger the stringent response and reconfigure cellular metabolism to adapt to challenging conditions to ensure bacterial survival (17–20). In addition, the stringent response plays a role in regulation of bacterial virulence and susceptibility to antimicrobials (18, 21–23). The stringent response pathway is characterized by the accumulation of guanosine tetra- (ppGpp) and pentaphosphate (pppGpp), collectively referred to as alarmones [(p)ppGpp]. In the majority of Gram-negative bacteria, these alarmones are produced by the synthetase RelA and hydrolyzed by SpoT. In these bacteria, binding of deacylated-tRNA to ribosomes activates alarmone production (24–27). In Gram-positive bacteria, these molecules are produced by a bifunctional RSH (RelA/SpoT homolog) protein, which possesses both alarmone synthetase and hydrolase activity (19, 28). Much less is understood about activation of the stringent response in Gram-positive bacteria. However, recent work in *Bacillus subtilis* suggests that alarmones target initiation factor 2 (IF2) and, in doing so, inhibit translation (29). Together, these data suggest a clear link between alarmones, tRNA targeting, and translation.

In this study, we show that MurMN is a molecular link between cell wall biosynthesis and translation quality control through its preferential utilization of misaminoacylated tRNA for the formation of indirect cross-links in pneumococcal peptidoglycan. Our findings indicate that the absence of these proteins sensitizes pneumococcal cells to acidic stress. Additionally, we found that a *murMN* deletion strain presents growth defects when grown in mildly acidic conditions, similar to those in which the ability of AlaRS to edit serine misaminoacylation of tRNA^{Ala} is reduced. The impairment of AlaRS editing activity likely resulted in the accumulation of mischarged tRNA and the subsequent activation of the stringent response pathway. Furthermore, our data suggest that activation of the stringent response is associated with the modulation of LytA activity, and this is reflected in changes in the initiation of stationary phase-induced autolysis and in the extent of phagocytosis of pneumococci. These findings provide insight into cell wall function by suggesting that cell wall biosynthesis enzymes can buffer the deleterious consequences of intracellular stress on protein synthesis and modulate entry into the stringent response pathway.

Results

The *murMN* Operon Protects Cells against Acid-Induced Growth Defects. When growing Δ*murMN* cells in planktonic culture, we observed a pronounced growth defect in rich media in mildly

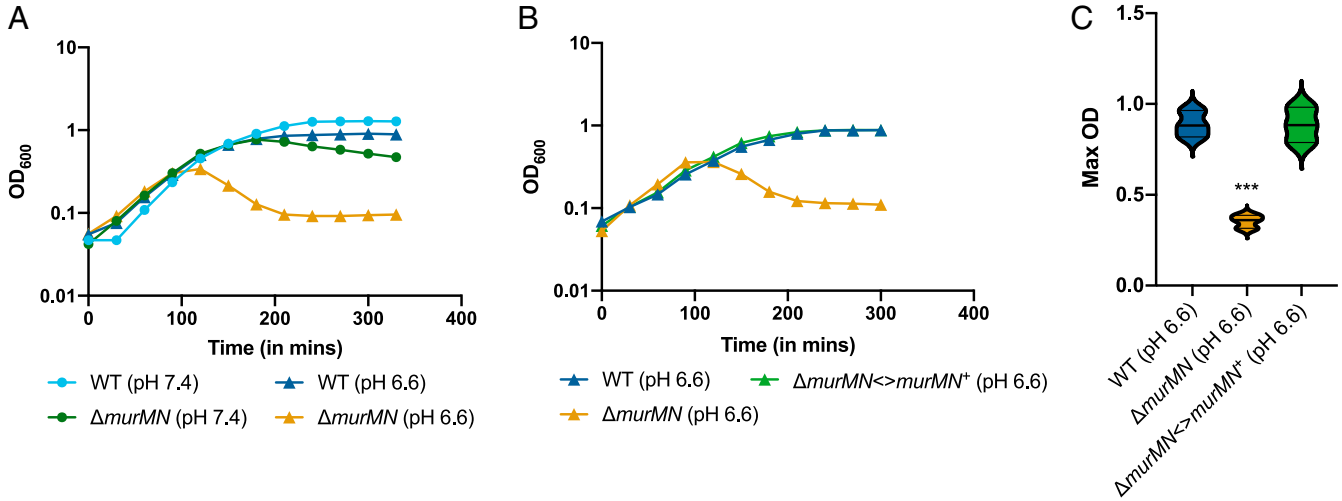

Fig. 1. Growth defects observed in the absence of *murMN*. (*A*) Representative growth curves for R6D wild-type and Δ*murMN* strains grown in normal (•) and acidic conditions (▲). (*B*) Representative growth curves comparing R6D Δ*murMN*<>*murMN*$^+$ growth with wild-type and Δ*murMN* strains grown in acidic conditions depicted in *A* (▲). (*C*) Violin plot depicting maximum growth of wild-type, Δ*murMN*, and Δ*murMN*<>*murMN*$^+$ strains grown in acidic conditions. Mean ± SD of max ODs: wild type (0.89 ± 0.07), Δ*murMN* (0.35 ± 0.04), and Δ*murMN*<>*murMN*$^+$ (0.88 ± 0.1). ***$P < 0.001$ relative to wild-type strain by ANOVA followed by Tukey's posttest. Growth curves were started at an OD_{600} of 0.05 (at least $n = 3$).

acidic conditions (pH 6.6) (Fig. 1*A*). The mutant exhibited increased susceptibility to stationary phase-induced autolysis and a decrease in the maximum optical density (max OD) reached during growth, consistent with growth arrest. This growth defect was rescued in a Δ*murMN* strain with a wild-type *murMN* knock-in (Δ*murMN*<>*murMN*$^{+}$) (Fig. 1 *B* and *C*). Although minor differences in growth of wild-type and Δ*murMN* strains were observed in rich media in normal conditions (pH 7.4), these differences were much more pronounced in mildly acidic conditions.

MurM and MurN contribute to cell wall branching by adding dipeptide cross-bridges to the peptidoglycan stem peptide that leads to production of branched muropeptides (8). The loss of branching alters pneumococcal cell wall composition and increases bacterial sensitivity to lysis by cell wall inhibitors (30). Thus, one hypothesis for the difference in sensitivity of wild-type and Δ*murMN* strains to acidic stress is that wild-type cells increase the number of cell wall bridges as a response to low pH and that the Δ*murMN* strain cannot mount this defense. To test this hypothesis, we employed high-performance liquid chromatography to analyze the peptidoglycan composition of pneumococci grown in rich media at normal (pH 7.4) and mildly acidic (pH 6.6) conditions for both wild-type and Δ*murMN* strains. We did not observe a significant difference in the extent of cross-links (direct or via cross-bridges) of the wild-type cells between normal and acidic conditions (Fig. 2 *A* and *B*, *i*). As expected, we observed that deletion of *murMN* led to the loss of branched peptides from the peptidoglycan as compared to wild-type cells (Fig. 2 *A* and *B*, *i*). Although the Δ*murMN* strain had a substantially higher number of direct cross-links, the total number of cross-links was not significantly different when this strain was grown at pH 6.6 or pH 7.4 (listed as monomers in Fig. 2 *B*, *i*). Similarly, the total number of cross-links was similar for the wild-type strain when grown at pH 6.6 or pH 7.4. Thus, the observation that the Δ*murMN* strain displays a pronounced growth defect at pH 6.6, but not at pH 7.4, could not be attributed to pH-dependent alterations in the extent of peptidoglycan cross-linking.

A second hypothesis for the difference in sensitivity of wild-type and Δ*murMN* strains to acidic stress is that the absence of cross-bridges in the Δ*murMN* peptidoglycan sensitizes the cell to LytA-mediated autolysis during log phase growth. Thus, we tested whether there was any difference in the sensitivity of wild-type and Δ*murMN* cells in log phase (when wild-type cells are refractory to LytA activity) grown in mildly acidic media to recombinant LytA (the major pneumococcal autolysin). Our data demonstrated that the absence of *murMN* did not increase the sensitivity of cells to autolysis by exogenously added LytA during log phase (Fig. 2*C*). We conclude that, relative to the wild type, the Δ*murMN* strain displays a growth defect in mildly acidic conditions and that this was not attributed to cell wall changes induced at the lower pH (as we did not detect changes in cell wall composition of wild-type cells between normal and mildly acidic pH) or to sensitivity to LytA-autolysis during log phase growth.

MurMN Attenuates Activation of the Stringent Response Pathway. The stringent response is a well-conserved pathway utilized by bacteria to ensure survival under stressed conditions. Mediated by the production of alarmones, the activation of this pathway reconfigures bacterial metabolism and coordinates cellular entry into stationary phase (17). We hypothesized that the differences in growth of the Δ*murMN* strain, relative to the wild-type strain,

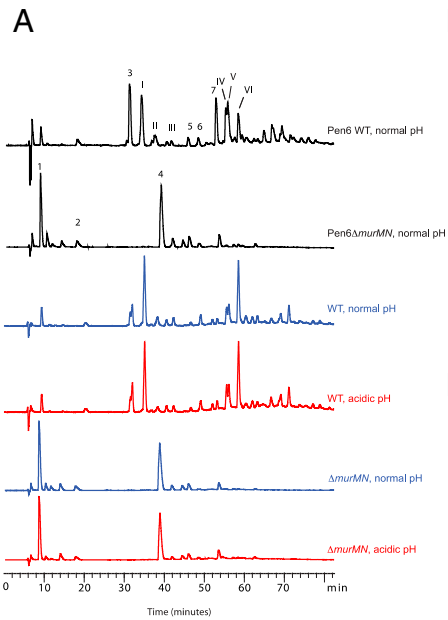

B i

Peptide	WT normal pH	WT acidic pH	ΔmurMN normal pH	ΔmurMN acidic pH	Pen6	Pen6ΔmurMN
1	4.5 (0.8)	5.3 (0.2)	41.1	38.0	3.4 (0.8)	28.7 (1.7)
2	1.5 (0.6)	1.7 (0.5)	4.5	3.3	1.4 (0.4)	12.5 (0.8)
3	8.5 (1.0)	10.1 (0.2)	0.0	0.0	19.5 (1.8)	0.6 (0.3)
I	27.4 (1.3)	25.1 (2.3)	0.0	0.0	16.1 (1.1)	0.4 (0.5)
II	4.2 (1.6)	3.1 (1.6)	0.1	0.0	9.2 (0.5)	0.0 (0.1)
III	4.9 (2.5)	4.8 (2.7)	0.0	0.0	4.8 (0.4)	2.5 (1.1)
4	1.4 (1.1)	1.5 (0.9)	44.7	46.6	0.2 (0.2)	31.4 (2.6)
5	1.3 (0.3)	1.6 (0.2)	5.6**	5.3**	2.7 (0.6)	11.0 (0.6)
6	3.2 (0.8)	3.8 (0.3)	0.8	2.4	1.9 (0.6)	1.2 (1.1)
7	2.6 (0.2)	3.1 (0.6)	0.1	0.3	13.6 (0.5)	8.0 (1.6)
IV	6.3 (0.7)	7.4 (0.8)	0.1	0.6	8.6 (0.4)	0.6 (0.5)
V	9.2 (0.2)	9.6 (0.8)	1.6	1.2	10.8 (0.6)	0.3 (0.2)
VI	24.8 (2.2)	23.1 (2.5)	1.4	2.3	7.9 (0.9)	2.7 (0.4)
Total Ser-Ala / Ala-Ala	0.344 (0.009)	0.391* (0.009)	NA	NA	1.35 (0.03)	NA
% Monomers	51.1 (3.5)	50.1 (5.5)	45.7	41.4	54.3 (2.5)	44.8 (1.0)

B ii

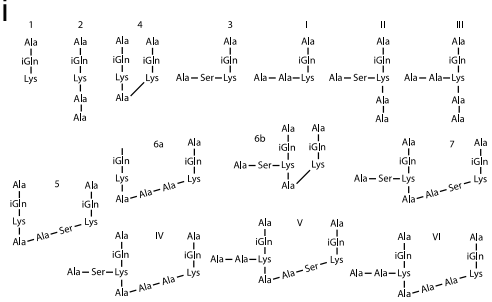

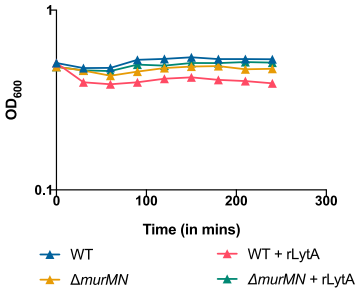

Fig. 2. Analysis of peptidoglycan structure of cells grown in normal and acidic conditions. (*A*) High-performance liquid chromatography profiles of the stem peptide compositions of peptidoglycan from strain R6D wild-type (WT) and R6D Δ*murMN* strain, grown in rich media in normal (blue) and mildly acidic (red) pH and harvested during exponential growth. In addition, strain Pen6 (WT and Δ*murMN*) is shown as a reference to identity key peaks (black) (*B*, *i*) Table presenting percentage and, in parentheses, the SD of each stem peptide structure in cell wall preparation from R6D strains grown in rich media at normal (blue) or mildly acidic (red) pH. Reference strain Pen6 (WT and Δ*murMN*) are shown in black. Summary rows present the average ratio (and SD) of total Ser–Ala to Ala–Ala under normal and mildly acidic pH and the average numbers of monomers (inverse measure of the level of peptidoglycan cross-linking). NA: nonapplicable. **P* < 0.05 relative to normal pH by unpaired Student's *t* test (at least *n* = 3, described in detail in *Materials and Methods*). (**) Composition of the corresponding peptide may not be identical to that of peak five from other strains (*B*, *ii*) Structures of the cell wall stem peptides that comprise pneumococcal peptidoglycan based on Pen6 references. (*C*) Representative curve depicting OD_{600} of R6D wild-type and Δ*murMN* cells harvested during the exponential phase in the absence or presence of 2 μg/mL recombinant LytA (at least *n* = 3).

was a consequence of activation of the stringent response pathway.

If activation of the stringent response pathway contributes to the low pH-induced early onset of stationary phase in Δ*murMN* pneumococci, this growth phenotype should be decreased or abrogated in a Δ*murMN* strain where the stringent response pathway cannot be activated. This pathway is activated by accumulation of the intracellular alarmones, ppGpp or pppGpp, which are hyperphosphorylated forms of guanosine 5′-diphosphate or guanosine 5′-triphosphate (GTP), respectively, synthesized by the addition of a pyrophosphate molecule obtained from adenosine 5′-triphosphate (ATP) (Fig. 3*A*). In the pneumococcus, the primary source of alarmone production is RSH, a bifunctional synthetase and hydrolase of (p)ppGpp (31). Thus, we deleted *rsh* (*spr_1487*) to generate strains defective in the ability to activate the stringent response pathway.

We compared growth among wild-type, Δ*rsh*, Δ*murMN*, and Δ*murMN*Δ*rsh* strains (Fig. 3*B*). The Δ*murMN*Δ*rsh* double mutant did not exhibit the growth defects observed for the Δ*murMN* strain in mildly acidic conditions. Thus, inhibition of the stringent response abrogates the growth defects in a Δ*murMN* background. To measure the relative alarmone levels in the Δ*murMN* strain relative to the wild-type strain in mildly acidic conditions, we employed thin-layer chromatography. The Δ*murMN* strain displayed increased alarmone levels compared to the wild-type strain, as observed by 2.5-fold higher levels of alarmone relative to GTP, congruent with growth defects in the absence of *murMN* (Fig. 3*C* and *SI Appendix*, Fig. S1). Furthermore, knock-in of Δ*murMN* pneumococci with wild-type *murMN* restored alarmone concentrations to those found in wild-type cells, while the Δ*rsh* mutants displayed very low levels of alarmone. We conclude that acidic conditions promote entry into stringent response and that MurMN attenuates the activation of stringent response and consequent entry into stationary phase.

Disruption of the Translation Quality Control Function of MurM Leads to Pneumococcal Growth Defects.

MurMN plays a role in correcting misaminoacylation of noncognate tRNA. How can a cell wall synthesis protein influence activation of the stringent response? We hypothesized that MurMN could be involved in the modulation of the stringent response due to its proposed role in the elimination of misacylated tRNAs.

MurM is an aminoacyl transferase that transfers L-serine or L-alanine from tRNAs to lipid II to ultimately form dipeptide cross-bridges in the peptidoglycan (8–10). The responsibility of ensuring fidelity of amino acid charging to their cognate tRNAs depends on the proofreading ability of aminoacyl-tRNA synthetases and, in many cases, on additional editing proteins that can reduce the number of misacylated tRNAs. For some aminoacyl-tRNA synthetases, errors resulting in aminoacylation of tRNA with noncognate amino acids are not uncommon (32). In fact, alanyl-tRNA^{Ala} synthetase (AlaRS), the enzyme responsible for charging tRNA^{Ala} to produce Ala-tRNA^{Ala}, is error prone, such that tRNA^{Ala} is often misacylated with serine (Ser-tRNA^{Ala}) or glycine (Gly-tRNA^{Ala}) (14, 15, 33).

Consistent with these observations, relative to cognate aminoacylation of tRNA^{Ala} with alanine, pneumococcal AlaRS generation of seryl-tRNA^{Ala} was easily detectable with high (8 μM) concentrations of AlaRS. However, we also observed that misaminoacylation of tRNA^{Ala} with glycine by this AlaRS was almost undetectable (*SI Appendix*, Fig. S2). These data suggested that the fidelity of pneumococcal protein synthesis was challenged by the aberrant amino acid specificity of AlaRS for serine. Therefore, if activation of the stringent response is sensitive to misacylated tRNAs, enzymes that decrease the number of misacylated tRNAs or that decrease errors in the aminoacylation of tRNAs would buffer entry into stringent response.

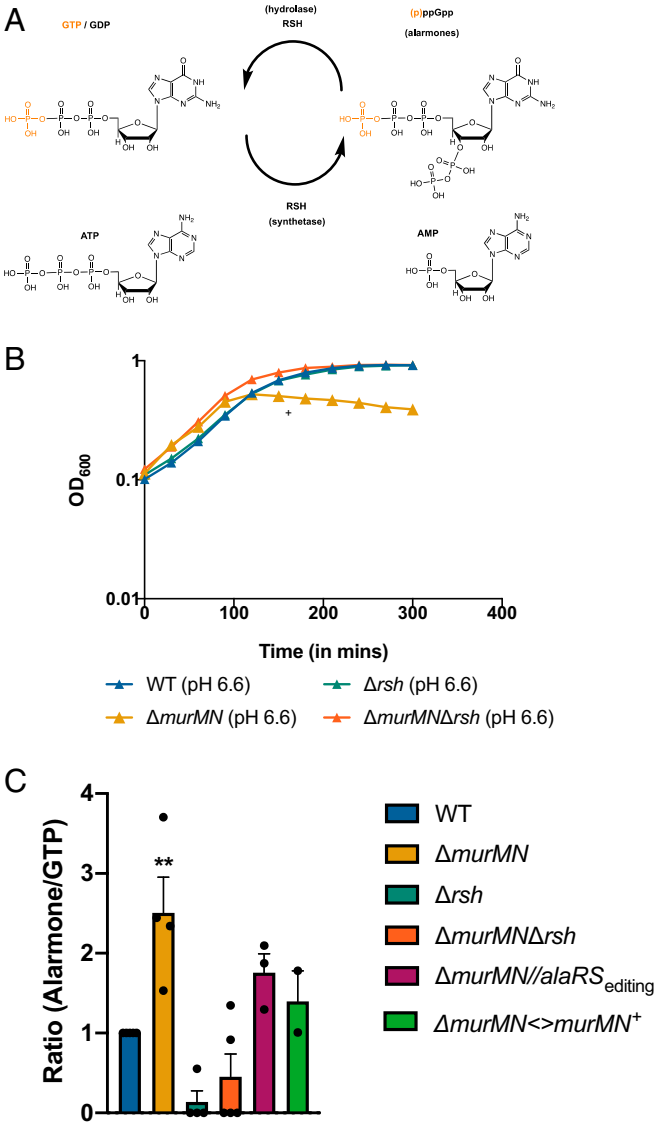

Fig. 3. MurMN attenuates entry into the stringent response pathway. (*A*) Schematic of (p)ppGpp synthesis and hydrolysis. (*B*) Representative growth curve for R6D wild-type, Δ*murMN*, Δ*rsh*, and Δ*murMN*Δ*rsh* strains grown in acidic conditions (▲). To circumvent the long lag phase of strains from Δ*rsh* background, strains were grown to log phase (~OD_{600} of 0.2) and collected by centrifugation and growth curves started at an OD_{600} of 0.1 (at least n = 3). (*C*) Ratios of alarmone ((p)ppGpp) to GTP as obtained by thin-layer chromatography in R6D wild-type, Δ*murMN*, Δ*rsh*, Δ*murMN*Δ*rsh*, Δ*murMN*//*alaRS*$_{editing}$, and Δ*murMN*<>*murMN*$^{+}$ strains grown in acidic conditions (n = 3, except for Δ*murMN*<>*murMN*$^{+}$ where n = 2) at pH 6.6. Measurements were made by harvesting cells in exponential phase. Bars represent average values with error bars denoting SEM values. $^{**}P < 0.01$ relative to wild-type strain by ANOVA followed by Tukey's posttest. Additionally, the ratio for Δ*murMN*Δ*rsh* is significantly different (P = 0.003) from that of Δ*murMN* strain.

Accumulation of Ser-tRNA^{Ala} is toxic to cells (14, 34), such that many organisms across all the three kingdoms of life encode AlaXp. This protein is homologous to the editing domain of the AlaRS protein and functions in hydrolytic editing of misaminoacylated tRNA^{Ala} to ensure fidelity of tRNA aminoacylation (35–39). The pneumococcus does not encode an AlaXp, and MurM has been proposed to fulfill this role (16). However, the catalytic turnover of seryl-tRNA^{Ala} hydrolysis by MurM has not been demonstrated, and there is no evidence for discrimination by MurM against utilizing cognate alanyl-tRNA^{Ala} (which are hydrolyzed

considerably faster than seryl-tRNA^{Ala}) (16). Nevertheless, it has been shown that MurM can utilize both alanyl-tRNA^{Ala} and seryl-tRNA^{Ser} species in the aminoacylation of peptidoglycan precursors (6). Therefore, as this enzyme recognizes both the aminoacyl and tRNA components of Ser-tRNA^{Ala}, we reasoned that MurM might fulfill this editing role through transfer of seryl groups from seryl-tRNA^{Ala} to lipid II-Lys. Therefore, we assessed the ability of recombinant MurM from different pneumococcal strains 159, 110K/70, and R6 to acylate lipid II-Lys with noncognate Ser-tRNA^{Ala} and compared it with the ability of these MurM enzymes to acylate lipid II with cognate substrates Ser-tRNA^{Ser} and Ala-tRNA^{Ala} (Fig. 4).

MurM$_{159}$ is identical in sequence to the MurM protein encoded by the *murMB1* allele expressed in strain R6D used in this work and is divergent in sequence (12% over protein sequence) from MurM$_{R6}$ encoded by *murMA* (6). For both alleles, dependencies of MurM lipid II aminoacylation activity on aminoacyl-tRNA concentration showed a high degree of selectivity for the misacylated seryl-tRNA^{Ala}. Using k_{cat}^{app}/K_m^{app} as a metric of catalytic efficiency, we found that seryl-tRNA^{Ala} was used as a substrate for aminoacylation of lipid II by MurM$_{159}$ and MurM$_{R6}$ 30.5-fold and 52.0-fold more efficiently than alanyl-tRNA^{Ala}, respectively. MurM$_{110K/70}$ [encoded by a *murMA* with single $V_{101} \rightarrow A_{101}$ mutation relative to the MurM$_{R6}$ *murMA* allele (40)] was similarly 61-fold more efficient in the utilization of seryl-tRNA^{Ala} relative to alanyl-tRNA^{Ala} (Fig. 4 and Table 1). We conclude that MurM derivatives that are produced by different pneumococcal clinical isolates can utilize seryl-tRNA^{Ala} considerably more efficiently than seryl-tRNA^{Ser} (Fig. 4).

These data suggest that in conditions where the levels of toxic Ser-tRNA^{Ala} accumulate, the cell wall may display an increase in Ser–Ala over Ala–Ala bridges within the peptidoglycan as it serves as a drainage system to use accumulating molecules of Ser-tRNA^{Ala}. In fact, we observed an increase in the ratio of total Ser–Ala/Ala–Ala within wild-type peptidoglycan in mildly acidic conditions relative to normal pH (Fig. 2 *B*, *i*). The high specificity with which MurM incorporates seryl-tRNA^{Ala} (relative to both seryl-tRNA^{Ser} and alanyl-tRNA^{Ala}), the absence of a gene encoding AlaXp in the pneumococcal genome, and an increase of serine in cell wall bridges in acidic versus normal conditions emphasize the importance of MurM within the context of peptidoglycan synthesis in translation quality control under certain conditions that stress pneumococci.

The efficiency of AlaRS editing is pH dependent. Deletion of *murMN* clearly abrogates the ability of the pneumococcus to correct misaminoacylation of noncognate tRNA, yet why would levels of misaminoacylation of tRNA^{Ala} be higher at a lower pH? We hypothesized that the strategies used by pneumococci to correct the misaminoacylation of tRNA^{Ala} were impaired. AlaRS avoids misaminoacylation of tRNA^{Ala} by hydrolysis of misactivated noncognate amino acyl adenylate to form 5′-AMP and noncognate amino acid prior to transfer of the aminoacyl group to the tRNA (pretransfer editing) or by hydrolysis of the noncognate aminoacyl-tRNA once this transfer has occurred (posttransfer editing) (*SI Appendix*, Fig. S3 *A* and *B*). Therefore, it was possible that amino acid lability of pre- or posttransfer editing by pneumococcal AlaRS could lead to an increase in misacylated tRNAs in the cell. To test this hypothesis, we devised a simple spectrophotometric method to follow the steady state proofreading rates of pre- (tRNA independent) and posttransfer (tRNA dependent) editing by AlaRS in acidic (pH 6.5) and normal (pH 7.6) conditions in the absence and presence of tRNA as a function of 5′-AMP release (*SI Appendix*, Fig. S3*C*). At either pH, addition of 5′-AMP to the assays led to an instantaneous consumption of all of the coupling enzyme system NADH substrate, indicating that pH does not impact the ability of the assay to follow AlaRS activity.

At pH 7.6, pretransfer editing in the presence of noncognate 100 mM L-serine was catalyzed by AlaRS at a rate of 2.15 ± 0.45 min^{-1}. Addition of 3.35 mg · mL^{-1} *Escherichia coli* crude tRNA, containing 2.12 μM tRNA^{Ala} isoacceptors, caused cycling of the tRNA pool between tRNA^{Ala} and seryl-tRNA^{Ala}. This registered as a pronounced 3.47-fold increase of 5′-AMP production to a posttransfer rate of seryl-tRNA^{Ala} editing of 5.32 ± 0.53 min^{-1} (Fig. 5 *A*, *i* and *ii*). Using a saturating concentration of the cognate amino acid L-alanine at 50 mM as a control, at pH 7.6, there was a much lower tRNA-independent turnover of alanyl-adenylate of 0.71 ± 0.12 min^{-1} and a negligible tRNA-dependent posttransfer rate (0.52 ± 0.09 min^{-1}) (Fig. 5 *B*, *i* and *ii*). To confirm that this assay did indeed follow posttransfer editing, we repeated these assays with AlaRS from which the posttransfer editing domain had been removed (AlaRS$_{(1-463)}$). Pretransfer editing of serine was still detectable (0.70 ± 0.08 min^{-1}); however, tRNA^{Ala} supported a posttransfer editing rate (0.49 ± 0.06 min^{-1}) that was less than pretransfer editing (Fig. 5 *A*, *iii*). These data were consistent with the ability of the tRNA-dependent 5′-AMP release assay to specifically follow AlaRS posttransfer editing.

On transition of AlaRS from pH 7.6 to 6.5, there was no significant drop in the rate of pretransfer serine editing, which was now 1.80 ± 0.07 min^{-1} (Fig. 5 *A*, *i* and *ii*). In contrast, at this lower pH, posttransfer serine editing was not stably maintained. Within 4 min of tRNA addition, this activity had decelerated to a steady state rate of 1.85 ± 0.49 min^{-1} that was equal to the rate of pretransfer editing and at this point was threefold less than the corresponding rate at pH 7.6 (Fig. 5 *A*, *i* and *ii*). When this experiment was repeated with alanine in place of serine at pH 6.5, there was a much lower

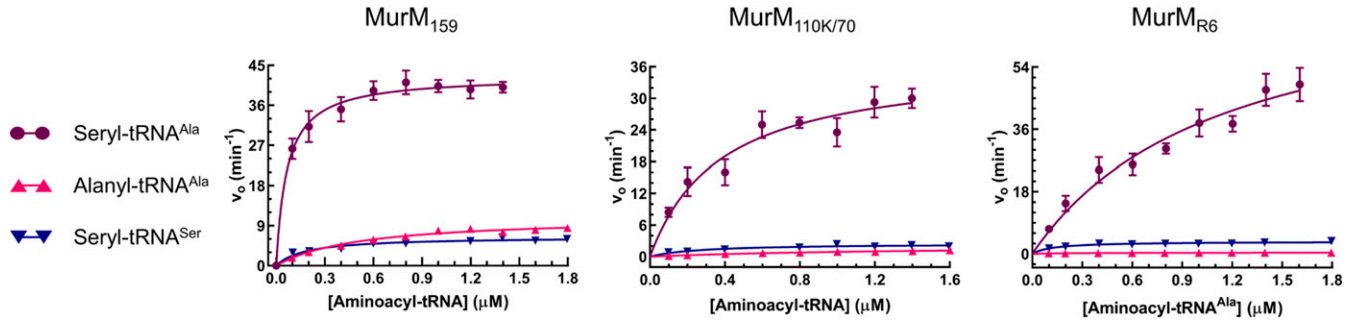

Fig. 4. Impact of misaminoacylation of tRNA on MurM-catalyzed aminoacylation of lipid II-Lys. Each MurM species was assayed at a constant concentration of 10 μM lipid II-Lys with increasing concentrations of [^{3}H]-seryl-tRNA^{Ala}, [^{3}H]-alanyl-tRNA^{Ala}, and [^{3}H]-seryl-tRNA^{Ser} at a specific activity of 100 cpm · pmol^{-1} in which pneumococcal tRNA$^{Ala}_{UGC}$ and tRNA$^{Ser}_{UGA}$ isoacceptors were employed. Respective MurM$_{159}$, MurM$_{110K/70}$, and MurM$_{R6}$ concentrations were 0.63, 2.00, and 1.00 nM in assays utilizing [^{3}H]-seryl-tRNA^{Ala}; 13, 91, and 126 nM in assays utilizing [^{3}H]-alanyl-tRNA^{Ala}; and 6, 18, and 11 nM in assays utilizing [^{3}H]-seryl-tRNA^{Ser}. Initial velocities of MurM activity (error bars represent variation between duplicate measurements) are plotted versus [aminoacyl-tRNA]. Data were fitted to the Michaelis–Menten equation using GraphPad Prism version 8.2.1.

Table 1. Catalytic efficiency of MurM encoded by three alleles, expressed as k_{cat}^{app}/K_m^{app}, relative to seryl-tRNA^{Ala}, seryl-tRNA^{Ser}, and alanyl-tRNA^{Ala}

MurM: Pneumococcal origin	Allele type	Aminoacyl-tRNA	K_m^{app} (μM)	k_{cat}^{app} (min^{-1})	k_{cat}^{app}/K_m^{app} ($min^{-1} \cdot \mu M^{-1}$)
159	*murMB1*	Alanyl-tRNA$^{Ala}_{UGC}$	0.5 ± 0.02	11 ± 0.53	22 ± 1.40
		Seryl-tRNA$_{UGA}^{Ser}$	0.2 ± 0.01	7 ± 0.30	31 ± 1.95
		Seryl-tRNA$^{Ala}_{UGC}$	***0.1 ± 0.01***	***42 ± 0.21***	***698 ± 116.44***
R6	*murMA*	Alanyl-tRNA$^{Ala}_{UGC}$	0.3 ± 0.02	0.4 ± 0.02	1.2 ± 0.10
		Seryl-tRNA$^{Ser}_{UGA}$	0.2 ± 0.01	4 ± 0.22	20 ± 1.55
		Seryl-tRNA$^{Ala}_{UGC}$	***1 ± 0.09***	***73 ± 7.34***	***77 ± 10.48***
110K/70	*murMA(V101 → A101)*	Alanyl-tRNA$^{Ala}_{UGC}$	1.3 ± 0.21	2 ± 0.19	2 ± 0.65
		Seryl-tRNA$^{Ser}_{UGA}$	0.3 ± 0.03	2 ± 0.06	9 ± 1.11
		Seryl-tRNA$^{Ala}_{UGC}$	***0.4 ± 0.08***	***37 ± 2.60***	***98 ± 32.56***

Bold italicized data correspond to those obtained with noncognate misaminoacylated seryl-tRNA$^{Ala}_{UGC}$.

tRNA-independent pretransfer turnover of alanyl-adenylate of 0.91 ± 0.09 min^{-1}, and as at pH 7.6, there was a residual tRNA-dependent posttransfer editing rate of 0.34 ± 0.05 min^{-1} (Fig. 5 *B*, *i* and *ii*). We therefore concluded that if intracellular pH is modified, the ability of pneumococcal AlaRS to support sustained elimination of seryl-tRNA^{Ala} is compromised (we discuss this data further in relation to mechanisms by which pH might impact AlaRS posttransfer editing and the impact of pH on the turnover of mis-serylated tRNAs in *SI Appendix*, *Supplemental Discussion of Figure 5*).

Overexpression of the editing domain of AlaRS can suppress the growth defect of ΔmurMN. The increased preference of MurM for mis-acylated tRNAs over correctly acylated tRNA species, combined with the drop of AlaRS editing efficiency caused by lowering pH, led us to propose that the growth phenotype of wild-type pneumococcus in acidic conditions resulted from compensation of the loss of translation quality control by MurM-catalyzed elimination of seryl-tRNA^{Ala}.

We reasoned that an increased expression of a tRNA-editing protein in a Δ*murMN* background could allow us to distinguish between the cell wall cross-linking and the translation quality control roles of MurM and therefore establish whether disruption of one or both of these roles was responsible for the growth defect of the Δ*murMN* strain. To this end, we identified the posttransfer editing domain of AlaRS encoded by pneumococcal *alaRS*

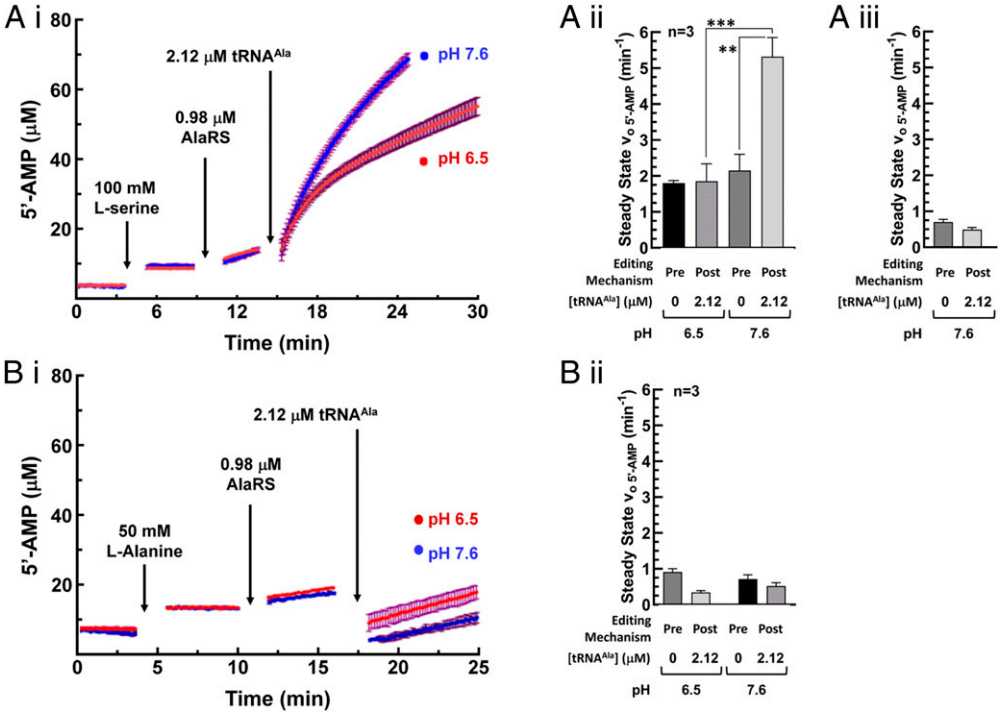

Fig. 5. Analysis of the impact of pH on serine editing by AlaRS. All assays were performed with AlaRS or its catalytic domain at an assay concentration of 0.98 μM. Absorbance data (340 nm) were converted to [5′-AMP] generated by editing. tRNA^{Ala} was added as constituent of a crude *E. coli* total tRNA preparation (Sigma) at a stock concentration 111.16 mg · mL^{-1} based on absorbance at 260 nm, containing 70.34 μM tRNA^{Ala} [all isoacceptors as assayed by aminoacylation with [^{3}H]-alanine, AlaRS, and trichloroacetic acid precipitation of the [^{3}H]-alanyl-tRNA^{Ala} product (6)] in which the final [tRNA^{Total}]$_{assay}$ and [tRNA^{Ala}]$_{assay}$ were 3.35 mg · mL^{-1} and 2.12 μM, respectively. All data are in triplicate with SDs. Posttransfer editing was calculated by subtraction of steady state rates in the presence of all components from rates without tRNA. Pretransfer editing rates were the difference between rates obtained in the absence of tRNA and the absence of AlaRS. (*A*) Pre- and posttransfer serine editing by *AlaRS* at pH 7.6 and 6.5: pH 6.5 data, red data points and purple error bars; pH 7.6 data, blue data points and purple error bars; (*A*, *i*) editing time course; (*A*, *ii*) AlaRS steady state serine editing rates where ***$P < 0.005$ and **$P < 0.02$ levels of significance in Student's *t* test comparisons; and (*A*, *iii*) AlaRS$_{(1\text{-}463)}$ steady state serine editing rates. (*B*) Pre- and posttransfer alanine editing *by AlaRS* at pH 7.6 and 6.5; (*B*, *i*) time course; (*B*, *ii*) AlaRS steady-state alanine editing rates.

(*spr_1240*) using an amino acid alignment with AlaRS proteins from *E. coli* (WP_096112793.1) and *B. subtilis* (WP_007408211.1), where the protein domains have been well characterized (36, 37, 41). The pneumococcal editing domain was therefore identified as residues 437 to 873 of the pneumococcal AlaRS, and this portion of the protein was used for functional complementation ($AlaRS_{editing}$) (Fig. 6*A*).

Ectopic expression of $AlaRS_{editing}$ is predicted to deacylate mischarged $tRNA^{Ala}$ species, the most abundant of which are Ser-$tRNA^{Ala}$ and Gly-$tRNA^{Ala}$ (16, 33, 34) (Fig. 6*B*). Since $AlaRS_{editing}$ only deacylates mischarged $tRNA^{Ala}$ molecules, its expression would not be expected to facilitate the correction of other erroneously alanylated or serylated tRNA species such as Ser-$tRNA^{Thr}$, Ala-$tRNA^{Pro}$, Ala-$tRNA^{Lys}$, or Ser-$tRNA^{Lys}$ synthesized by the class II synthetases (32, 42) (ThrRS, LysRS, or ProRS) (orange in Fig. 6*B*).

The expression of $AlaRS_{editing}$ in the Δ*murMN* strain partially rescued the growth defect displayed by this strain in mildly acidic conditions (Fig. 6*C*). Specifically, the Δ*murMN*//*alaRS*$_{editing}$ strain resembled the wild type in that it did not exhibit the dramatically increased stationary phase-induced lysis associated with the Δ*murMN* strain, and the max OD achieved by this strain was intermediate between the Δ*murMN* and wild-type strains. Finally, we tested whether the expression of $AlaRS_{editing}$ in Δ*murMN* also influenced alarmone levels, and as predicted by our model, the levels of alarmome in the Δ*murMN*//*alaRS*$_{editing}$ strain resembled that of the wild type (Fig. 3*C*). These findings illustrate the importance of MurM consumption of misacylated tRNA species in vivo and imply that MurM ensures normal growth in mildly acidic conditions by its ability to consume toxic and mischarged tRNAs through peptidoglycan precursor acylation. Moreover, we conclude that in the absence of MurMN, the accumulation of misacylated tRNA species triggers the stringent response.

MurMN Dampens LytA-Mediated Lysis. The role of MurMN in preventing activation of the stringent response pathway via its ability to deacylate mischarged tRNAs explains the growth arrest described in Fig. 1. Next, we questioned the mechanism responsible for the increased lysis subsequent to growth arrest observed in the Δ*murMN* strain when grown in mildly acidic conditions (Fig. 1). Having established that MurMN influences activation of the stringent response pathway, we searched for the molecule(s) responsible for the autolysis. Autolysis of pneumococcal cells is carried out by autolysins, peptidoglycan hydrolases containing choline-binding domains that enable their binding to phosphocholine residues present on the teichoic acids of the cell wall (43–45). The addition of exogenous choline inhibits this binding and the consequent autolysis (43, 46–48). The addition of choline chloride (final concentration of 2% [weight/volume]) to Δ*murMN* grown in mildly acidic conditions abrogated lysis, suggesting lysis is triggered by choline-binding autolysins (Fig. 7 *A*, *i*). Of the multiple choline-binding proteins encoded in the pneumococcal genomes, LytA is the major autolysin. To investigate whether the increased lysis of Δ*murMN* is induced by LytA, we tested growth of Δ*murMN* with a deletion in *lytA* (Δ*murMN*Δ*lytA*). The double mutant resembled the wild-type strain in that it did not display lysis (Fig. 7 *A*, *ii*). Importantly, the lower maximal OD observed in the Δ*murMN* strain was not restored to wild-type levels in the Δ*murMN*Δ*lytA* strain. This rescue of only the lysis phenotype suggests that in the absence of MurMN, activation of the stringent response may induce early onset of stationary phase and that LytA is responsible for the subsequent autolysis phenotype. The dramatically increased sensitivity of the Δ*murMN* strain to LytA activity, relative to both the wild-type strain at mildly acidic pH and the Δ*murMN* strain in normal conditions, suggest that MurMN is positively associated with the activation of LytA under mildly acidic conditions. The autolytic activity of LytA is linked to stationary phase onset (49, 50), and thus, we propose that early entry into the stationary phase may be a trigger for LytA.

MurMN Impacts Macrophage Phagocytosis by Influencing LytA Activity. Pneumococcal cells encounter numerous environmental stresses in an infection setting. Among these is acidic pH, encountered as a result of the inflammatory response mounted by the host against the invading bacteria (51, 52). Previous work suggests that LytA contributes to pneumococcal evasion from phagocytosis (53), and our data revealed that Δ*murMN* cells display increased activation of LytA activity. Thus, we hypothesized that macrophages would be less efficient at uptake of Δ*murMN* pneumococci relative to wild-type cells.

Since the capsule is a major contributor to the evasion of cells from phagocytosis, we moved to the encapsulated strain D39 (serotype 2 strain, which is the ancestor of R6D strain) to test whether MurMN influenced macrophage phagocytosis of pneumococci.

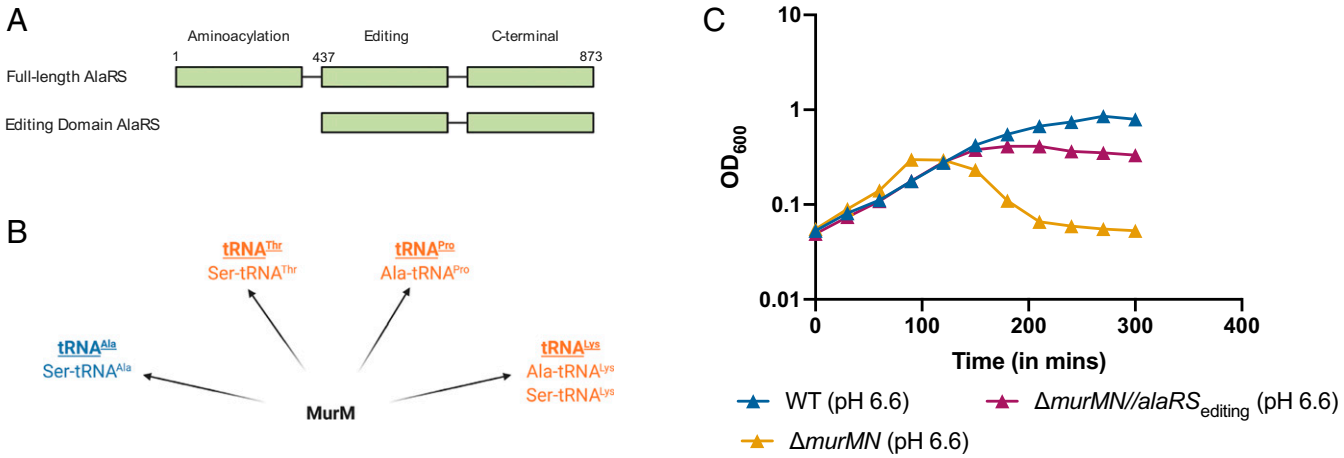

Fig. 6. Analysis of translation quality control function of MurM (*A*) Schematic representation of the domain architecture of full-length and ectopically expressed editing domains of AlaRS. (*B*) Schematic represents the various naturally mischarged species that MurM is likely to encounter (underlined). AlaRS can misaminoacylate $tRNA^{Ala}$ with Ser, ThrRS can misaminoacylate $tRNA^{Thr}$ with Ser, ProRS can misaminoacylate $tRNA^{Pro}$ with Ala, and LysRS can misaminoacylate $tRNA^{Lys}$ with Ala and Ser. Expression of $AlaRS_{editing}$ protein can deacylate mischarged $tRNA^{Ala}$ (blue). Other mischarged tRNA moieties cannot be corrected by $AlaRS_{editing}$ protein (orange). Schematic based on findings from previous work (16, 32–34, 41). (*C*) Representative growth curve for R6D wild-type and isogenic Δ*murMN* and Δ*murMN*//*alaRS*$_{editing}$ strains grown in acidic conditions (▲). Growth curves were started at an OD_{600} of 0.05 (at least $n = 3$).

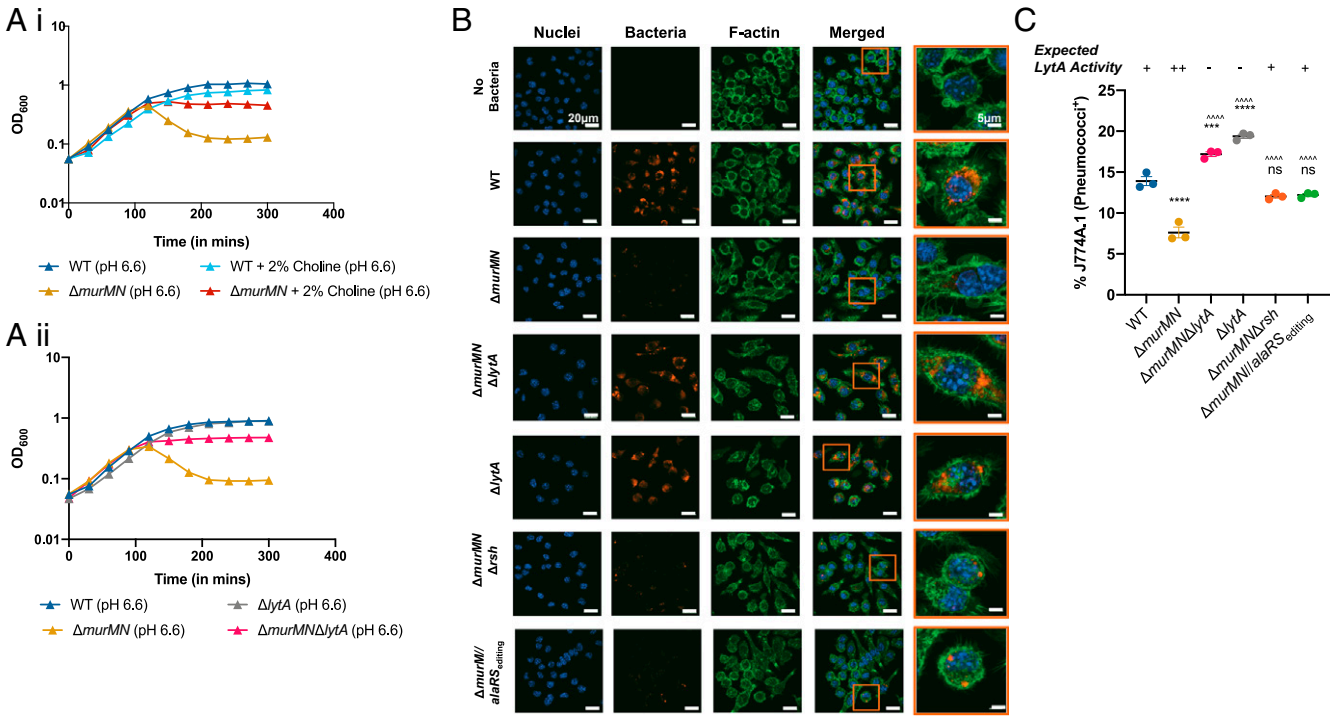

Fig. 7. MurMN influences LytA-mediated phenotypes. (*A*) LytA-mediated autolysis is triggered in Δ*murMN* cells. (*A*, *i*) Representative growth curve for R6D wild-type and Δ*murMN* strains grown in acidic conditions (▲), either in the absence or presence of 2% (wt/vol) choline chloride. Growth curves were started at an OD_{600} of 0.05. (*A*, *ii*) Representative growth curve for R6D wild-type, Δ*murMN*, Δ*lytA*, and Δ*murMN*Δ*lytA* strains grown in acidic conditions (▲). Growth curves were started at an OD_{600} of 0.05 (at least $n = 3$). Mean ± SD of max ODs: wild type (0.89 ± 0.07), Δ*murMN* (0.35 ± 0.04), and Δ*murMN*Δ*lytA* (0.52 ± 0.1). (*B* and *C*) MurMN controls LytA-mediated evasion from phagocytosis. Internalization of pneumococcal cells (in a D39 background) with J774A.1 macrophages. (*B*) Confocal microscopy images depicting bacterial internalization after 60 min. In blue: macrophage nuclei, red: bacterial cells, and green: actin. The rightmost column of images represents magnified areas from the inset marked by red squares in the column depicting merged channels. (*C*) Quantification of J774A.1 macrophages positive for pneumococci after 30 min, as separated by flow cytometry. "ns" denotes nonsignificant comparisons, ***$P < 0.001$, and ****$P < 0.0001$ relative to wild type; ^^^^$P < 0.0001$ relative to Δ*murMN* by ANOVA followed by Tukey's posttest. The graph also shows expected LytA activity for each strain, "+" denotes basal levels, "++" denotes increased levels, and "-" denotes absence.

The number of macrophages positive for pneumococci was about twofold lower when infected with Δ*murMN* relative to the wild-type strain (Fig. 7 *B* and *C* and *SI Appendix*, Fig. S4). Furthermore, this phenotype was reversed for the Δ*murMN*Δ*lytA* strain, demonstrating the importance of LytA to this phenotype (Fig. 7 *B* and *C*). Finally, in agreement with previous work (53), the number of macrophages positive for pneumococcus was increased upon infection with a Δ*lytA* strain relative to the wild type (Fig. 7 *B* and *C*).

Our data suggest that the activation of LytA in the Δ*murMN* strain requires activation of the stringent response pathway. Thus, if a Δ*murMN* strain does not induce the stringent response, it should not display increased evasion from macrophages. In support of this contention, the number of macrophages that internalized the Δ*murMN*Δ*rsh* strain was higher than those that internalized the Δ*murMN* strain. Finally, our model predicts that MurMN buffers the stringent response and LytA-mediated autolysis via its role in deacylating the misacylated tRNAs. Consistently, we observed a higher number of macrophages positive for the Δ*murMN*//*alaRS*$_{editing}$ strain relative to the Δ*murMN* strain (Fig. 7 *B* and *C*). These data are consistent with a role for MurMN in activation of the stringent response and subsequent increase in LytA activity and reveal the consequence of MurMN-mediated stringent response suppression for phagocytosis.

The decreased percentage of macrophages positive for Δ*murMN* pneumococci could be a consequence of either greater pneumococcal evasion of phagocytosis or increased lysis of pneumococcal cells upon their internalization by macrophages (where the pH of phagolysosomes is much lower than the pH 6.6 used in our studies). If the acidic environment of macrophages promotes increased lysis of the Δ*murMN* pneumococci, there should be a rapid decrease in internalized bacteria over time. In contrast, we observe a more gradual decline in internalized Δ*murMN* pneumococcus relative to wild-type cells (*SI Appendix*, Fig. S5). Thus, the Δ*murMN* strain appears to evade phagocytosis, and, as previously reported, this process is LytA dependent (53).

Discussion

Elucidating the mechanisms that bacterial cells employ to compartmentalize their functions or organize cell-wide responses to environmental stresses is of fundamental interest to the field of microbiology. The staphylococci have evolved mechanisms to partition cognate aminoacylated tRNA molecules between translation and cell wall biosynthesis. For instance, *Staphylococcus aureus* encodes a set of isoacceptor $tRNA^{Gly}$ species that display a greater propensity for biosynthesis of peptidoglycan than for protein synthesis via diminished binding to the EF-Tu elongation factor utilized in translation (54–56). Similarly, *Staphylococcus epidermidis* contains a $tRNA^{Ser}$ and two $tRNA^{Gly}$ species that are only competent in peptidoglycan synthesis (56–58). In contrast, in other bacterial species, the same pool of aminoacyl-tRNAs is assumed to serve both purposes of peptidoglycan modification and translation (54). The tRNA-dependent amino acyl transferases MurM and MurN are involved in pneumococcal cell wall biosynthesis: they build dipeptide cross-bridges that serve as a major component of the bacterial cell wall and contribute to penicillin resistance. Here, we demonstrate that in doing so, one such enzyme, MurM, resolves the threat that tRNA misaminoacylation posed to protein synthesis by utilizing misaminoacylated

tRNA to aminoacylate peptidoglycan precursors with remarkable specificity.

We found that three enzymes encoded by different *murM* alleles use noncognate misaminoacylated seryl-tRNA^{Ala} to serylate the peptidoglycan precursor lipid II-Lys with up to 20-fold greater catalytic efficiency than either correctly aminoacylated cognate alanyl-tRNA^{Ala} or seryl-tRNA^{Ser}. This strongly suggests that MurM can attenuate intracellular stress through preferential sequestration of incorrectly aminoacylated tRNA into peptidoglycan synthesis. It has been proposed that MurM acts to preserve fidelity of protein synthesis through catalyzing the simple hydrolysis of misaminoacylated tRNA (16). However, this was based upon assays where enzyme to seryl- or alanyl-tRNA^{Ala} ratios were 10,000:1 (16) and could not therefore address the catalytic properties of MurM. In contrast, our MurM lipid II-Lys aminoacylation assays were performed with enzyme:seryl-tRNA^{Ala} ratios of less than 1 in 50 in which product accumulation always exceeded the concentration of MurM. Additionally, the previously reported rate of deacylation of alanyl-tRNA^{Ala} by MurM was greater than the rate of seryl-tRNA^{Ala} deacylation, inconsistent with the proposed role of MurM in the control of the fidelity of protein biosynthesis (16). In contrast, and consistent with its proposed role, we found that MurM was considerably more specific for the misaminoacylated seryl-tRNA^{Ala} than the cognate alanyl-tRNA^{Ala}. Finally, hydrolytic deacylation of alanyl-tRNA^{Ala} by MurM was negligible compared to rates of aminoacylation of peptidoglycan precursors (6). These observations lead us to conclude that the most likely mechanism by which MurM corrects AlaRS editing deficiencies is by incorporation of misdirected seryl residues into the pneumococcal peptidoglycan.

In vivo, our analysis of cell wall composition is consistent with functional MurM leading to an increased amount of seryl residues in peptidoglycan dipeptide branches at pH 6.5 compared to 7.6. This fits a model where MurM acts to consume misaminoacylated tRNA generated by a diminution of the ability of AlaRS (and perhaps ThrRS) to carry out effective posttransfer editing at a reduced pH. Pneumococcal isolates display-wide variation in the extent and composition of the branched muropeptides within their peptidoglycan (11). We suggest that stresses such as, but not limited to, pH on editing by aminoacyl-tRNA synthetases contribute to this variability.

There are precedents from several lactic acid bacteria that low pH conditions trigger a drop in internal pH, allowing these cells to maintain a constant pH gradient across the membrane. For example, in *Streptococcus thermophilus*, reduction in external pH between 7 and 5 is mirrored by reduction in intracellular pH to as low as pH 5.5 (59). Similarly, in *Streptococcus bovis*, an external pH range of 5.4 to 6.5 translates to an internal pH of 5.5 to 6.7; this maintains a constant ΔpH across the cell membrane and forestalls toxic accumulations of fermentation product anions (60, 61). Furthermore, *Streptococcus mutans* with a glucose energy source maintain a pH gradient across the cell membrane, which dissipates on exhaustion of the carbon source and depletion of ATP (62). Therefore, for *S. pneumoniae*, which can generate up to 35 mM D-lactic acid from the fermentation of glucose (63), it is likely that this organism also meets the challenge of acidic growth conditions by optimizing the pH gradient across its cytoplasmic membrane through reduction of its intracellular pH. On exhaustion of the carbon source, and entry into stationary phase, it is likely that the pneumococcal intracellular pH will fall. We did not confirm the intracellular pneumococcal pH relative to the corresponding external pH. However, it seems likely that the drop in external pH may have induced a drop in intracellular pH (before or on consumption of the pneumococcal carbon source), which compromised translational fidelity via decreased editing by AlaRS (Fig. 5). During pneumococcal infection, this effect may be exacerbated in the phagosomal environment, where the pH in the phagosomal lumen can be as low as 4.5 (64). The heterogeneity of cell wall composition that results from these stresses may make peptidoglycan an environmentally sensitive readout of the response of MurM activity to variable levels of mischarged seryl-tRNAs.

A drop in intracellular pH and consequent decreased editing of AlaRS provides one hypothesis for the increased level of mischarged seryl-tRNAs. Another hypothesis is that the drop in extracellular pH impacts the function of an extracellular protein. For instance, if decreased pH impacts the activity of penicillin binding proteins (PBPs), this could induce a stress response. In support of this, there is an association between pH and pneumococcal cell shape (65), and in *E. coli*, PBP function is dependent on pH (66).

The posttransfer editing domain of AlaRS is functional in the absence of the N-terminal tRNA aminoacylation domain of the enzyme (37). We used this functionality to confirm that the increase in seryl-tRNA^{Ala} because of the absence of MurMN was a cause of acid stress-induced early onset of stationary phase. We suggest that, in the Δ*murMN* strain, this construct augmented the compromised editing capacity of AlaRS at this pH, allowing sufficient restoration of editing activity to consume seryl-tRNA^{Ala} that would have been utilized by MurM in the wild-type pneumococcus.

However, overexpression of the posttransfer editing domain of pneumococcal AlaRS as a seryl-tRNA^{Ala} deacylase in our Δ*murMN* strain only partially reversed its growth deficit at acidic pH. This could be related to levels of expression or activity of the AlaRS posttransfer editing domain. Alternatively, the incomplete restoration of growth at the lower pH might also be the result of impaired ThrRS posttransfer editing in these conditions (67), which would not have been reversed by overexpression of the posttransfer editing domain of AlaRS. Additionally, if a component of the acid-sensitive Δ*murMN* phenotype was contributed by an impediment to PBP-catalyzed peptidoglycan transpeptidation at low pH, this could similarly also account for the partial reversal of this phenotype by expression of the editing domain of AlaRS.

Our results further revealed that in addition to suppression of seryl-tRNA^{Ala} accumulation through expression of MurM or the posttransfer editing domain of AlaRS, the acid-sensitive growth phenotype of Δ*murMN* strains could be reversed by deletion of *rsh*, which reduced alarmone synthesis and therefore suppressed activation of the stringent response. Furthermore, alarmone levels were inversely related to expression of *murMN*. This suggested that there is a causal link between misaminoacylated tRNA accumulation and activation of the pneumococcal stringent response. It therefore seems that in order to prevent potential corruption of translation, consumption of seryl-tRNA^{Ala} by MurM may represent a first line of defense. When this mechanism is overwhelmed (or as here, absent in Δ*murMN*), the stringent response shuts down translation to avoid further toxic generation of mistranslated/misfolded protein (*SI Appendix*, Fig. S6).

In summary, our studies in the pneumococcus revealed that in the absence of MurM, the accumulation of mischarged tRNAs (possibly via pH-induced diminution of posttransfer editing by AlaRS) initiates the stringent response, premature entry into stationary phase, and subsequent activation of the murein hydrolase LytA. In this context, the cell wall biosynthesis protein MurM, by virtue of its role in preferentially using mischarged seryl-tRNA^{Ala} to aminoacylate peptidoglycan precursors, dampens activation of the stringent response and calibrates the cellular reaction to this stress.

An outstanding question in this model is how do mischarged tRNAs accumulated because of the absence of MurM trigger the stringent response? Binding of aminoacyl-tRNA to the ribosomal A-site provides the required amino acid for polypeptide elongation (19). In Gram-negative bacteria, binding of deacylated tRNAs to the ribosome activates RelA and induces alarmone production (19). Activation of the stringent response is

MICROBIOLOGY

less understood in Gram-positive bacteria, where the alarmone synthetase and hydrolase functions are fused in the bifunctional RSH enzyme (17, 68, 69). Our data, which suggests an accumulation of mischarged tRNAs concurrent with initiation of RSH-catalyzed alarmone production to trigger the stringent response in pneumococcus, could indicate that RSH may be activated by binding of mischarged tRNAs to the ribosome.

A second hypothesis is that the stringent response is activated by unfolded proteins. In the case of seryl-tRNA^{Ala} accumulation through mutation of AlaRS posttransfer editing domains (34, 70), and in other examples of unrestrained tRNA mischarging (71), errors in protein synthesis accumulate and account for substantial losses of cellular viability. The production of mistranslated proteins leads to up-regulation of the heat shock response genes *rpoH*, *dnaK*, and *mopA* in *E. coli* (71, 72). In this context, it is interesting to note that (p)ppGpp accumulation has recently been shown to be an integral part of the Firmicute heat shock response of *Bacillus subtilis* (73). Therefore, we propose that a deficit in pneumococcal translational quality control caused by the absence of MurM activity and pH-driven attenuation of posttransfer editing by AlaRS, and possibly ThrRS, generates sufficient seryl-tRNA$^{Ala/Thr}$ to overwhelm the capacity of pretransfer editing to prevent access of these noncognate species into protein synthesis. The consequential generation of misfolded protein arising from substitution of serine for alanine at GCN codons triggers (p)ppGpp accumulation by RSH, which inhibits translation IF2 (29), thereby attenuating protein synthesis and transitioning the organism into a quiescent state and therefore triggering the stringent response to cause cessation of growth.

Consistent with its role in the response to stress, RSH is the main source of pneumococcal alarmone and in the nutritional stringent response, provides increased fitness in cells subjected to mupirocin, an antibiotic that causes increasing cellular levels of deacylated tRNA^{Ile}. Additionally, RSH is a virulence determinant in murine models of pneumococcal pneumonia and sepsis and promotes resistance to killing by neutrophils to provide a fitness advantage in a murine model of colonization (31, 74). Together, these studies strongly suggest that the ability of the pneumococcus to trigger the stringent response is critical for virulence. We therefore propose that MurMN plays a role in delaying or fine-tuning entry into the stringent response and as such, may contribute to the outcome of pneumococcal infections. The ability of MurMN to forestall acid-induced entrance into the stringent response on phagocytosis is likely to play a role in macrophage survival during pathogenesis.

In eukaryotes, prokaryotes, and the archaea, AlaXp proteins are conserved in their ability to deacylate seryl-tRNA^{Ala} but not necessarily glycyl-tRNA^{Ala}, which has recently been shown to be deacylated by D-aminoacyl–tRNA deacylase (38, 80). Similarly, here we showed that pneumococcal AlaRS misaminoacylation of tRNA^{Ala} with glycine is negligible compared to that with serine, a characteristic also shared by eukaryotic AlaRSs (34). This, in addition to the specificity of D-aminoacyl–tRNA deacylase, suggests that unlike seryl-tRNA^{Ala}, glycyl-tRNA^{Ala} doesn't accumulate enough to threaten fidelity of protein synthesis that MurM is required to correct. Consistent with this hypothesis, pneumococcal peptidoglycan cell wall bridges do not contain glycine (11).

Deacylating mischarged tRNA^{Ala} is crucial, wherein accumulation of seryl-tRNA^{Ala} is toxic and where even partial diminution of posttransfer editing of this species has pathological consequences (33, 67). It has been proposed that AlaXp is an evolutionary solution to the ubiquitous challenge of Ser-tRNA^{Ala} production (38). We suggest that MurM is an alternative evolutionary solution to this challenge during conditions of cellular stress.

Genomic analysis reveals that many Firmicutes encoding cell wall tRNA-dependent aminoacyl transferases that produce peptide bridges do not appear to encode for an AlaXp protein. These include the following: *Staphylococcus aureus*, *Staphylococcus epidermidis*, *Streptococcus thermophilus*, *Streptococcus agalactiae*, *Streptococcus salivarius*, *Enterococcus faecalis*, and *Weissella viridescens* (75). It is therefore tempting to speculate that cell wall bridges containing proteogenic amino acids may reflect the function of cell wall tRNA-dependent aminoacyl transferase in translation quality control. Consistent with this hypothesis, Firmicutes that encode AlaXp proteins include *Bacillus subtilis* and *Bacillus megaterium*, which have no cell wall bridges, and *Enterococcus faecium*, *Pediococcus pentosaceus*, and *Lactobacillus cellobiosus* (syn. *fermentans*), which do have cell wall bridges but those that are composed of nonproteogenic D-*iso*-asparagine. We contend that these species encode AlaXp proteins to carry out the role performed by MurM and its homologs in other Firmicutes (75–77).

In conclusion, this study suggests that MurM provides a molecular link between cell wall biosynthesis and translation quality control in *S. pneumoniae* that produce short peptide bridges in their peptidoglycan layer. These bridges are structural components that contribute to antibiotic resistance (8–10, 13). This study provides in vivo evidence to suggest that the propensity of MurM to utilize mischarged tRNA allows it to serve as a translation quality control checkpoint and dampen entry into the stringent response. Through these mechanisms, MurM influences the activity of LytA and phagocytosis. These findings implicate MurM and therefore peptidoglycan synthesis in the survival of bacteria as they encounter unpredictable and hostile conditions in the host. The question of how the regulation of these fundamental biological processes by MurM influences the extent of pathogenesis still remains to be investigated. Our work provides functional insight into the role of peptidoglycan peptide bridge-generating enzymes in modulating intracellular stress and entry into the stringent response.

Materials and Methods

Growth Curves. Strains of interest were streaked on TSA II agar plates supplemented with 5% (volume/volume [vol/vol]) sheep blood. These streaked cells were then inoculated into fresh Columbia broth (normal or acidic) and incubated at 37 °C and 5% (vol/vol) CO_2 without shaking. Once the cultures reached an OD_{600} of 0.05, the growth of the cultures was followed every 30 min by recording their optical density at a wavelength of 600 nm.

Strains with a Δ*rsh* genetic background showed a much longer lag phase. To circumvent this, when comparing growth of cells with strains in Δ*rsh* background, we adapted our protocol from a previous study measuring growth of these cells (31). The cells were grown in acidic Columbia broth to an OD_{600} of ∼0.2. The cells were then collected by centrifugation at 3,000 rpm for 10 min and resuspended in acidic Columbia broth to an OD_{600} of ∼0.1. The growth of these cultures at 37 °C and 5% (vol/vol) CO_2 without shaking was followed every 30 min by recording their optical density at 600 nm.

All strains whose growth curves are represented in a given figure panel were grown in the same batch of media. The replicates were performed with fresh preparations of media on different days.

AlaRS Serine Editing Assays. AlaRS editing assays were performed to follow serine- and tRNA-dependent generation of 5′-AMP at 37 °C in a continuous coupled assay in a final volume of 0.2 mL containing 50 mM Hepes, pH 7.6, or 50 mM 3-(*N*-morpholino)propanesulfonic acid, pH 6.5, 10 mM $MgCl_2$, 50 mM KCl, 1 mM dithiothreitol, 2 mM ATP, 2 mM phosphoenol pyruvate, 0.3 mM NADH, 40 mM · min^{-1} rabbit muscle myokinase, 8 mM · min^{-1} rabbit muscle pyruvate kinase, and 11.5 mM · min^{-1} rabbit muscle lactate dehydrogenase. Absorbance was followed in triplicate at 340 nm (OD_{340}) in a Cary 100 UV-Vis double beam spectrophotometer for 3 min, at which point assays were supplemented with 100 mM L-serine. To initiate pretransfer editing, 0.98 μM AlaRS was added to the cuvette, and 5′ AMP generated by seryl-adenylate formation and hydrolysis was followed as a drop in OD_{340}. To initiate posttransfer editing, 3 mg · mL^{-1} crude *E. coli* tRNA comprising 2.12 μM tRNA^{Ala} isoacceptors [assayed by [^{3}H]-L-alanine aminoacylation of tRNA with *S. pneumoniae* AlaRS according to Lloyd et al. (6)] were added to the cuvette. The 5′-AMP additionally generated from the continual formation and hydrolysis of seryl-tRNA^{Ala} was then followed as a drop in OD_{340}. Assays were additionally performed in which L-serine was replaced by

L-alanine and 5′-AMP concentration was determined assuming consumption of two equivalents of NADH/5′-AMP in which for NADH, $\varepsilon_{1cm,\ 340\ nm}$ = 6,220 $M^{-1} \cdot cm^{-1}$.

AlaRS tRNA^{Ala} Aminoacylation Assays. Aminoacylation of crude *S. pneumoniae* 159 tRNA [prepared as previously described (6)] was followed at 37 °C in 0.1 mL by incubation of 2.12 mg · mL^{-1} tRNA in 30 mM Hepes, 15 mM $MgCl_2$, 10 mM dithiothreitol, 2 mM ATP, pH 7.6, 2 mM · min^{-1} inorganic pyrophosphatase, 8.2 μM $AlaRS_{159}$, and 37.5 μM (18.53 μCi/mL) [^{3}H]-L-alanine, L-serine, or glycine. 10 μL samples were taken over 60 min and [^{3}H]-aminoacyl-tRNA was estimated from precipitation of radioactivity onto Whatman 3 mm paper as previously described (6). Equivalent control assays were run in the absence of tRNA.

MurM Aminoacyl Transferase Assays. MurM assays following the production of [^{3}H]-seryl-lipid II-Lys or [^{3}H]-alanyl-lipid II-Lys were conducted as described (6) at a constant concentration of 10 μM lipid II-Lys. For all MurM proteins, the aminoacyl-tRNA concentration ranges over which MurM was assayed were 0.1 μM to 1.8 μM (both [^{3}H]-seryl-tRNA^{Ser} and [^{3}H]-alanyl-tRNA^{Ala}) and 0.1 μM to 1.6 μM for [^{3}H]-seryl-tRNA^{Ala}. All assays carried out with [^{3}H]-alanyl-tRNA and [^{3}H]-seryl-tRNAs also contained 1 mM L-alanine or 1 mM L-serine. The respective $MurM_{159}$, $MurM_{110K/70}$, and $MurM_{R6}$ assay concentrations were 0.63, 2.00, and 1.00 nM in assays utilizing [^{3}H]-seryl-tRNA^{Ala}; 13, 91, and 126 nM in assays utilizing [^{3}H]-alanyl-tRNA^{Ala}; and 6, 18, and 11 nM in assays utilizing [^{3}H]-seryl-tRNA^{Ser}. All data were collected from 2 min of incubations, for which it could be established that MurM-catalyzed accumulation of product was linear with respect to time. In all cases, assay response was linearly related to [MurM]. Data were fitted to the Michaelis–Menten equation using GraphPad Prism 8.2.1 (GraphPad Software, Inc.).

Other Methods. Additional methods not described here are included in *SI Appendix, Supplemental Materials & Methods*.

Data Availability. All study data are included in the article and/or supporting information.

ACKNOWLEDGMENTS. We thank Prof. Alexander Tomasz for introducing us to the study of MurMN through stimulating discussions and challenging questions. We also thank him for providing the R6D strain used in this study. We thank Rory Eutsey for his assistance with laboratory experiments, Dr. Aaron Mitchell for productive advice throughout the development of this project, and Drs. John Woolford and Elaine Tuomanen for insightful discussions during the writing and revision of this manuscript. This work was supported by NIH Grant R00-DC-011322 to N.L.H. and the Stupakoff Scientific Achievement Award and Glen de Vries Presidential Fellowship to S.D.A. The work also received support from the Eberly Family Trust and the Department of Biological Sciences at Carnegie Mellon University. S.R.F. was supported by Portuguese national funds from a PTDC/BIA-MIC/30746/2017 research grant, from the UCIBIO research unit, UID/Multi/04378/2019, and from the ONEIDA (an omics network to prevent and control infectious diseases and antimicrobial resistance) project (LISBOA-01-0145-FEDER-016417). C.G.D., A.J.L., and D.I.R. were funded through Medical Research Council Grants G0400848, G1100127, and MR/N002679/1 to C.G.D. The funders had no role in study design, data collection and analyses, decision to publish, or preparation of the manuscript.

1. T. J. Silhavy, D. Kahne, S. Walker, The bacterial cell envelope. *Cold Spring Harb. Perspect. Biol.* **2**, a000414 (2010).
2. M. Rajagopal, S. Walker, Envelope structures of Gram-positive bacteria. *Curr. Top. Microbiol. Immunol.* **404**, 1–44 (2017).
3. A. L. Koch, Bacterial wall as target for attack: Past, present, and future research. *Clin. Microbiol. Rev.* **16**, 673–687 (2003).
4. V. Sukhithasri, N. Nisha, L. Biswas, V. Anil Kumar, R. Biswas, Innate immune recognition of microbial cell wall components and microbial strategies to evade such recognitions. *Microbiol. Res.* **168**, 396–406 (2013).
5. A. Tomasz, Surface components of *Streptococcus pneumoniae*. *Rev. Infect. Dis.* **3**, 190–211 (1981).
6. A. J. Lloyd *et al*., Characterization of tRNA-dependent peptide bond formation by MurM in the synthesis of *Streptococcus pneumoniae* peptidoglycan. *J. Biol. Chem.* **283**, 6402–6417 (2008).
7. G. De Pascale *et al*., Kinetic characterization of lipid II-Ala:alanyl-tRNA ligase (MurN) from *Streptococcus pneumoniae* using semisynthetic aminoacyl-lipid II substrates. *J. Biol. Chem.* **283**, 34571–34579 (2008).
8. S. R. Filipe, A. Tomasz, Inhibition of the expression of penicillin resistance in *Streptococcus pneumoniae* by inactivation of cell wall muropeptide branching genes. *Proc. Natl. Acad. Sci. U.S.A.* **97**, 4891–4896 (2000).
9. S. R. Filipe, E. Severina, A. Tomasz, Functional analysis of *Streptococcus pneumoniae* MurM reveals the region responsible for its specificity in the synthesis of branched cell wall peptides. *J. Biol. Chem.* **276**, 39618–39628 (2001).
10. S. R. Filipe, M. G. Pinho, A. Tomasz, Characterization of the *murMN* operon involved in the synthesis of branched peptidoglycan peptides in *Streptococcus pneumoniae*. *J. Biol. Chem.* **275**, 27768–27774 (2000).
11. S. R. Filipe, E. Severina, A. Tomasz, Distribution of the mosaic structured *murM* genes among natural populations of *Streptococcus pneumoniae*. *J. Bacteriol.* **182**, 6798–6805 (2000).
12. A. M. Smith, K. P. Klugman, Alterations in MurM, a cell wall muropeptide branching enzyme, increase high-level penicillin and cephalosporin resistance in *Streptococcus pneumoniae*. *Antimicrob. Agents Chemother.* **45**, 2393–2396 (2001).
13. A. M. Smith, K. P. Klugman, Non-Penicillin-Binding protein mediated high-level penicillin and cephalosporin resistance in a Hungarian clone of *Streptococcus pneumoniae*. *Microb. Drug Resist.* **6**, 105–110 (2000).
14. K. Beebe, L. Ribas De Pouplana, P. Schimmel, Elucidation of tRNA-dependent editing by a class II tRNA synthetase and significance for cell viability. *EMBO J.* **22**, 668–675 (2003).
15. M. Guo, P. Schimmel, Structural analyses clarify the complex control of mistranslation by tRNA synthetases. *Curr. Opin. Struct. Biol.* **22**, 119–126 (2012).
16. J. Shepherd, M. Ibba, Lipid II-independent *trans* editing of mischarged tRNAs by the penicillin resistance factor MurM. *J. Biol. Chem.* **288**, 25915–25923 (2013).
17. K. Potrykus, M. Cashel, (p)ppGpp: Still magical? *Annu. Rev. Microbiol.* **62**, 35–51 (2008).
18. K. Poole, Bacterial stress responses as determinants of antimicrobial resistance. *J. Antimicrob. Chemother.* **67**, 2069–2089 (2012).
19. V. Hauryliuk, G. C. Atkinson, K. S. Murakami, T. Tenson, K. Gerdes, Recent functional insights into the role of (p)ppGpp in bacterial physiology. *Nat. Rev. Microbiol.* **13**, 298–309 (2015).
20. K. Liu, A. N. Bittner, J. D. Wang, Diversity in (p)ppGpp metabolism and effectors. *Curr. Opin. Microbiol.* **24**, 72–79 (2015).
21. Z. D. Dalebroux, S. L. Svensson, E. C. Gaynor, M. S. Swanson, ppGpp conjures bacterial virulence. *Microbiol. Mol. Biol. Rev.* **74**, 171–199 (2010).
22. Z. D. Dalebroux, M. S. Swanson, ppGpp: Magic beyond RNA polymerase. *Nat. Rev. Microbiol.* **10**, 203–212 (2012).
23. E. Maisonneuve, K. Gerdes, Molecular mechanisms underlying bacterial persisters. *Cell* **157**, 539–548 (2014).
24. W. A. Haseltine, R. Block, Synthesis of guanosine tetra- and pentaphosphate requires the presence of a codon-specific, uncharged transfer ribonucleic acid in the acceptor site of ribosomes. *Proc. Natl. Acad. Sci. U.S.A.* **70**, 1564–1568 (1973).
25. F. S. Pedersen, E. Lund, N. O. Kjeldgaard, Codon specific, tRNA dependent in vitro synthesis of ppGpp and pppGpp. *Nat. New Biol.* **243**, 13–15 (1973).
26. T. M. Wendrich, G. Blaha, D. N. Wilson, M. A. Marahiel, K. H. Nierhaus, Dissection of the mechanism for the stringent factor RelA. *Mol. Cell* **10**, 779–788 (2002).
27. R. M. Knutsson Jenvert, L. Holmberg Schiavone, Characterization of the tRNA and ribosome-dependent pppGpp-synthesis by recombinant stringent factor from *Escherichia coli*. *FEBS J.* **272**, 685–695 (2005).
28. G. C. Atkinson, T. Tenson, V. Hauryliuk, The RelA/SpoT homolog (RSH) superfamily: Distribution and functional evolution of ppGpp synthetases and hydrolases across the tree of life. *PLoS One* **6**, e23479 (2011).
29. S. Diez, J. Ryu, K. Caban, R. L. Gonzalez Jr., J. Dworkin, The alarmones (p)ppGpp directly regulate translation initiation during entry into quiescence. *Proc. Natl. Acad. Sci. U.S.A.* **117**, 15565–15572 (2020).
30. S. R. Filipe, E. Severina, A. Tomasz, The *murMN* operon: A functional link between antibiotic resistance and antibiotic tolerance in *Streptococcuspneumoniae*. *Proc. Natl. Acad. Sci. U.S.A.* **99**, 1550–1555 (2002).
31. K. M. Kazmierczak, K. J. Wayne, A. Rechtsteiner, M. E. Winkler, Roles of rel(Spn) in stringent response, global regulation and virulence of serotype 2 Streptococcus pneumoniae D39. *Mol. Microbiol.* **72**, 590–611 (2009).
32. J. Ling, N. Reynolds, M. Ibba, Aminoacyl-tRNA synthesis and translational quality control. *Annu. Rev. Microbiol.* **63**, 61–78 (2009).
33. W.-C. Tsui, A. R. Fersht, Probing the principles of amino acid selection using the alanyl-tRNA synthetase from *Escherichia coli*. *Nucleic Acids Res.* **9**, 4627–4637 (1981).
34. J. W. Lee *et al*., Editing-defective tRNA synthetase causes protein misfolding and neurodegeneration. *Nature* **443**, 50–55 (2006).
35. P. Schimmel, Mistranslation and its control by tRNA synthetases. *Philos. Trans. R. Soc. Lond. B Biol. Sci.* **366**, 2965–2971 (2011).
36. I. Ahel, D. Korencic, M. Ibba, D. Söll, Trans-editing of mischarged tRNAs. *Proc. Natl. Acad. Sci. U.S.A.* **100**, 15422–15427 (2003).
37. K. Beebe, M. Mock, E. Merriman, P. Schimmel, Distinct domains of tRNA synthetase recognize the same base pair. *Nature* **451**, 90–93 (2008).
38. Y. E. Chong, X.-L. L. Yang, P. Schimmel, Natural homolog of tRNA synthetase editing domain rescues conditional lethality caused by mistranslation. *J. Biol. Chem.* **283**, 30073–30078 (2008).
39. M. Guo *et al*., Paradox of mistranslation of serine for alanine caused by AlaRS recognition dilemma. *Nature* **462**, 808–812 (2009).
40. J. Shepherd, *Characterisation of Pneumococcal Peptidoglycan Cross-Linking Enzymology* (University of Warwick, 2011).
41. M. Guo *et al*., The C-Ala domain brings together editing and aminoacylation functions on one tRNA. *Science* **325**, 744–747 (2009).
42. H. Jakubowski, Misacylation of tRNA^{Lys} with noncognate amino acids by lysyl-tRNA synthetase. *Biochemistry* **38**, 8088–8093 (1999).

43. S. Giudicelli, A. Tomasz, Attachment of pneumococcal autolysin to wall teichoic acids, an essential step in enzymatic wall degradation. *J. Bacteriol.* **158**, 1188–1190 (1984).
44. K. K. Gosink, E. R. Mann, C. Guglielmo, E. I. Tuomanen, H. R. Masure, Role of novel choline binding proteins in virulence of *Streptococcus pneumoniae*. *Infect. Immun.* **68**, 5690–5695 (2000).
45. B. Maestro, J. M. Sanz, Choline binding proteins from *Streptococcus pneumoniae*: A dual role as enzybiotics and targets for the design of new antimicrobials. *Antibiotics (Basel)* **5**, 21 (2016).
46. J.-V. Höltje, A. Tomasz, Lipoteichoic acid: A specific inhibitor of autolysin activity in Pneumococcus. *Proc. Natl. Acad. Sci. U.S.A.* **72**, 1690–1694 (1975).
47. T. Briese, R. Hakenbeck, Interaction of the pneumococcal amidase with lipoteichoic acid and choline. *Eur. J. Biochem.* **146**, 417–427 (1985).
48. J. L. Garcia, E. Diaz, A. Romero, P. Garcia, Carboxy-terminal deletion analysis of the major pneumococcal autolysin. *J. Bacteriol.* **176**, 4066–4072 (1994).
49. P. Mellroth *et al*., LytA, major autolysin of *Streptococcus pneumoniae*, requires access to nascent peptidoglycan. *J. Biol. Chem.* **287**, 11018–11029 (2012).
50. J. Flores-Kim, G. S. Dobihal, A. Fenton, D. Z. Rudner, T. G. Bernhardt, A switch in surface polymer biogenesis triggers growth-phase-dependent and antibiotic-induced bacteriolysis. *eLife* **8**, e44912 (2019).
51. A. Lardner, The effects of extracellular pH on immune function. *J. Leukoc. Biol.* **69**, 522–530 (2001).
52. S.-Y. Park, I.-S. Kim, Identification of macrophage genes responsive to extracellular acidification. *Inflamm. Res.* **62**, 399–406 (2013).
53. E. Ramos-Sevillano *et al*., Pleiotropic effects of cell wall amidase LytA on *Streptococcus pneumoniae* sensitivity to the host immune response. *Infect. Immun.* **83**, 591–603 (2015).
54. M. Raina, M. Ibba, tRNAs as regulators of biological processes. *Front. Genet.* **5**, 171 (2014).
55. R. M. Bumsted, J. L. Dahl, D. Söll, J. L. Strominger, Biosynthesis of the peptidoglycan of bacterial cell walls. X. Further study of the glycyl transfer ribonucleic acids active in peptidoglycan synthesis in Staphylococcus aureus. *J. Biol. Chem.* **243**, 779–782 (1968).
56. R. J. Roberts, Staphylococcal transfer ribonucleic acids. II. Sequence analysis of isoaccepting glycine transfer ribonucleic acids IA and IB from Staphylococcus epidermidis Texas 26. *J. Biol. Chem.* **249**, 4787–4796 (1974).
57. J.-F. Petit, J. L. Strominger, D. Söll, Biosynthesis of the peptidoglycan of bacterial cell walls. VII. Incorporation of serine and glycine into interpeptide bridges in Staphylococcus epidermidis. *J. Biol. Chem.* **243**, 757–767 (1968).
58. T. S. Stewart, R. J. Roberts, J. L. Strominger, Novel species of tRNA. *Nature* **230**, 36–38 (1971).
59. H. Siegumfeldt, K. Björn Rechinger, M. Jakobsen, Dynamic changes of intracellular pH in individual lactic acid bacterium cells in response to a rapid drop in extracellular pH. *Appl. Environ. Microbiol.* **66**, 2330–2335 (2000).
60. G. M. Cook, J. B. Russell, The effect of extracellular pH and lactic acid on pH homeostasis in *Lactococcus lactis* and *Streptococcus bovis*. *Curr. Microbiol.* **28**, 165–168 (1994).
61. J. B. Russell, F. Diez-Gonzalez, The effects of fermentation acids on bacterial growth. *Adv. Microb. Physiol.* **39**, 205–234 (1998).
62. Y. Iwami *et al*., Intracellular and extracellular pHs of *Streptococcus mutans* after addition of acids: Loading and efflux of a fluorescent pH indicator in streptococcal cells. *Oral Microbiol. Immunol.* **17**, 239–244 (2002).
63. L. Paixão *et al*., Transcriptional and metabolic effects of glucose on Streptococcus pneumoniae sugar metabolism. *Front. Microbiol.* **6**, 1041 (2015).
64. A. Haas, The phagosome: Compartment with a license to kill. *Traffic* **8**, 311–330 (2007).
65. A. J. Perez *et al*., Movement dynamics of divisome proteins and PBP2x:FtsW in cells of *Streptococcus pneumoniae*. *Proc. Natl. Acad. Sci. U.S.A.* **116**, 3211–3220 (2019).
66. E. A. Mueller, A. J. F. Egan, E. Breukink, W. Vollmer, P. A. Levin, Plasticity of *Escherichia coli* cell wall metabolism promotes fitness and antibiotic resistance across environmental conditions. *eLife* **8**, e40754 (2019).
67. W. F. Waas, P. Schimmel, Evidence that tRNA synthetase-directed proton transfer stops mistranslation. *Biochemistry* **46**, 12062–12070 (2007).
68. K. Braeken, M. Moris, R. Daniels, J. Vanderleyden, J. Michiels, New horizons for (p)ppGpp in bacterial and plant physiology. *Trends Microbiol.* **14**, 45–54 (2006).
69. C. Wolz, T. Geiger, C. Goerke, The synthesis and function of the alarmone (p)ppGpp in firmicutes. *Int. J. Med. Microbiol.* **300**, 142–147 (2010).
70. Y. Liu *et al*., Deficiencies in tRNA synthetase editing activity cause cardioproteinopathy. *Proc. Natl. Acad. Sci. U.S.A.* **111**, 17570–17575 (2014).
71. T. J. Bullwinkle, M. Ibba, Translation quality control is critical for bacterial responses to amino acid stress. *Proc. Natl. Acad. Sci. U.S.A.* **113**, 2252–2257 (2016).
72. S. Gottesman, Genetics of proteolysis in *Escherichia coli*. *Annu. Rev. Genet.* **23**, 163–198 (1989).
73. H. Schäfer *et al*., The alarmones (p)ppGpp are part of the heat shock response of *Bacillus subtilis*. *PLoS Genet.* **16**, e1008275 (2020).
74. Y. Li *et al*., Identification of pneumococcal colonization determinants in the stringent response pathway facilitated by genomic diversity. *BMC Genomics* **16**, 369 (2015).
75. K. H. Schleifer, O. Kandler, Peptidoglycan types of bacterial cell walls and their taxonomic implications. *Bacteriol. Rev.* **36**, 407–477 (1972).
76. W. Staudenbauer, J. L. Strominger, Activation of D-aspartic acid for incorporation into peptidoglycan. *J. Biol. Chem.* **247**, 5095–5102 (1972).
77. W. Staudenbauer, E. Willoughby, J. L. Strominger, Further studies of the D-aspartic acid-activating enzyme of Streptococcus faecalis and its attachment to the membrane. *J. Biol. Chem.* **247**, 5289–5296 (1972).